Fibrin-bound thrombin determines clot structure and blood thrombogenicity in normofibrinogenemia and dysfibrinogenemia

Siyu Sun,[1] Mark Roest,[1] Rolf T. Urbanus,[2] Elena Campello,[3] Sarah Beck,[4] Cristiana Bulato,[3] Simon D. Connell,[5] Philip G. de Groot,[1] Timea Feller,[6] Dana Huskens,[1] Joke Konings,[1] Rita Marchi,[7] Harmen Middelveld,[1] Patricia Öftering,[4] Bernhard Nieswandt,[4] Alessandro Casini,[7] Robert A. S. Ariëns,[6] Paolo Simioni,[3] Johan W. M. Heemskerk[1] and Bas de Laat[1]

[1]Synapse Research Institute Maastricht, Maastricht, the Netherlands; [2]Van Kreveldkliniek, University Medical Center Utrecht, the Netherlands; [3]Department of Medicine, University of Padua, Padova, Italy; [4]Rudolf Virchow Center for Integrative and Translational Bioimaging and Institute of Experimental Biomedicine, Julius-Maximilians-Universität Würzburg, Würzburg, Germany; [5]Molecular and Nanoscale Physics Group, School of Physics, University of Leeds, Leeds, UK; [6]Discovery and Translational Science Department, Leeds Institute of Cardiovascular and Metabolic Medicine, University of Leeds, Leeds, UK and [7]Division of Angiology and Hemostasis, Department of Medicine, University Hospitals of Geneva, University of Geneva, Geneva, Switzerland

Correspondence: M. Roest
M.Roest@thrombin.org

Received: July 1, 2025.
Accepted: January 26, 2026.
Early view: February 5, 2026.

https://doi.org/10.3324/haematol.2025.288585

Abstract

In thrombosis and hemostasis, coagulation and platelet activation pathways culminate to form solid fibrin clots, which can become vaso-occlusive or prevent excessive bleeding. We report a novel mechanism describing how developing fibrin clots prolong and modulate the reactivity of thrombin, an enzyme propagating platelet and coagulation activation and forming fibrin from fibrinogen. Using immunological and genetic approaches, we delineate how thrombin bound to the Aα and Bβ chains of fibrin E-domains regulates lateral fibrin fiber extension. Our data reveal that fibrin-bound thrombin remains active and is temporarily protected against inactivation by antithrombin-III. Immunological displacement of thrombin from fibrin profoundly lowered its capacity, whereas a peptide mimicking the Aα-chain binding-site increased its reactivity. In a cohort of patients with congenital dysfibrinogenemia, carrying *FGA, FGB* or *FGG* mutations associated with bleeding or thrombosis phenotypes, we noticed a high thrombin capacity and suppressed thrombin-antithrombin-III complex formation, pointing to a prolonged active thrombin lifetime, likely due to abnormal formation of thrombin-containing fibrin. In conclusion, the combination of impaired clotting and increased thrombogenicity may explain the paradoxical bleeding and thrombotic complications observed in such patients. Development of fibrin-directed agents may offer new therapeutic opportunities to normalize hemostasis or prevent thrombosis.

Introduction

Coagulation operates as a cascade-based process that involves intricate interplays of coagulant and anticoagulant factors in blood plasma as well as platelets, red blood cells and leukocytes, with modulatory actions by endothelial and smooth muscle cells in the vessel wall.[1-3] A key proteolytic enzyme in coagulation is thrombin, which is generated from prothrombin on procoagulant membranes, such as highly activated platelets. Extrinsic thrombin generation is triggered by subendothelial tissue factor (TF), while negatively charged surfaces trigger the process via the intrinsic contact activation pathway.[4] First traces of generated thrombin activate platelets via G-protein-coupled receptors, whereas nanomolar levels of thrombin need to be generated to cleave plasma fibrinogen molecules to produce insoluble fibrin meshes or clots.[5,6] The latter proteolytic action of thrombin consists of N-terminal cleavage of fibrinopeptide A (FpA, 16 amino acids) from two fibrinogen Aa-chains, and slower N-terminal cleavage of fibrinopeptide B (FpB, 14 amino acids) from two fibrinogen Bβ-chains.[7,8] A range of heterozygous mutations in the three fibrinogen-encoding genes, *FGA, FGB* and *FGG*, associates with dysfibrinogenemia, where carrying subjects can be asymptomatic or in one-third to one-sixth of cases encounter bleeding or thrombotic events.[9] While their hemostatic impairment

is usually explained by the quantitative and qualitative fibrinogen defects, underlying causes of the thrombosis risk are not well understood.

The fibrin monomers firstly formed by thrombin consist of so-called D-E-D domains, which then assemble as half-staggered oligomers to polymerize into laterally extending, elastic fibrin fibres.[10,11] In coagulating blood, the result is a stable clot or thrombus, consisting of fibrin matrix and contracting platelets.[12] A crystal structure revealed in 2004 that the E-domain-thrombin complex consists of two thrombin molecules, primarily bound via the exosite-I and interacting with N-terminal regions of the cleaved Aα- and Bβ-chains.[13] Still unknown is the fate of this medium-affinity thrombin pool. In contrast, well resolved in later studies is the thrombogenic role of high-affinity binding site of thrombin to a splice variant of fibrinogen g, known as fibrinogen g-prime (g').[14]

In the present manuscript, we employed fibrin-targeted single chain antibodies and fibrin-mimicking peptides as well as advanced biophysical investigations to unravel the reactivity, lifetime and role of the Aα/Bβ-chain fibrin-bound thrombin. We report high levels of this active thrombin pool, which control the process of thrombin generation under conditions of normo- and dysfibrinogenemia. We further provide new evidence for high coagulant activity in patients with congenital dysfibrinogenemia. Unlike the early designations of fibrin as antithrombin-I,[15] we now postulate that fibrin acts as a protective thrombin shield for antithrombin-III capturing.

Methods

A full description of materials, experimental procedures and statistical analysis is provided in the *Online Supplementary Appendix*.

Human blood donors

Studies with blood from healthy donors were approved by the Medical Ethical Committee of Maastricht University Medical Center (NL31480.068.10) and were conducted according to the Declaration of Helsinki. Patient studies were approved by the Research and Ethics Committees of Padua University Hospital Italy (protocol code 4303/AO17, July 28, 2017) and of the University Hospitals of Geneva (Switzerland). Studies were conducted in accordance with the Declaration of Helsinki. Blood donors had not taken anticoagulant or antiplatelet medication for 2 weeks and gave written informed consent. Congenital dysfibrinogenemia was classified from reduced fibrinogen activity level in comparison to the antigen level. Genotyping followed the International Society of Thrombosis and Hemostasis classification. Screenings for *FGA, FGB* and *FGG* mutations were based on suspected dysfibrinogenemia, and were performed by polymerase chain reaction amplification of fibrinogen coding sequences and Sanger sequencing.[16] For subject cohort testing, plasmas were obtained from 64 healthy individuals (see *Online Supplementary Appendix*). Included were samples from 28 males and 36 females, with a median age of 34 and 32 years, respectively. Preparation procedures of blood, platelet-rich plasma (PRP) and isolated plasma are described in the *Online Supplementary Appendix*.

Thrombin generation and thrombin pool assessments

Thrombin generation measurements were performed within 96-well-plates at 37°C, employing a low-affinity fluorogenic substrate for thrombin not interfering with the coagulation process, as described for plasma[17] and whole blood.[18]

To quantify the effect of Nb106 on thrombin activity in TF-triggered plasma over time, we calculated the average thrombin lifetime, defined as the ratio of the total amount of thrombin generated during 60 minutes (endogenous thrombin potential or ETP until the end of the curve, expressed as nM x min) to the amount of prothrombin consumed in this interval. The TF-triggered prothrombin consumption over 60 minutes was measured with a staphylocoagulase assay, as described in the *Online Supplementary Appendix*. Calculations of the fibrin-(in)dependent thrombin pools and the average thrombin lifetime are also detailed in the *Online Supplementary Appendix*. The term thrombin capacity refers to a plasma coagulation phenotype, distinct from the thrombin generation (TG) curve parameter ETP, as it reflects the overall ability of plasma to generate thrombin in response to a specific trigger rather than the integrated amount of thrombin formed over time.

Coagulation measurements

Clotting times, clot turbidity and clot contraction measurements as well as fibrinogen function and antigen levels were determined, as described in the *Online Supplementary Appendix*.

Advanced microscopy

Atomic force microscopy was employed as before for high-resolution imaging of fibrin protofibril and fibril assembly.[19] Multicolour fluorescence and confocal microscopy were used to monitor platelet-dependent coagulation in whole blood under conditions of flow (wall-shear rates 200 and 1,000 s^{-1}), as described for mouse blood[20] and human blood.[21]

Thrombin-antithrombin complex assessment

Thrombin-antithrombin (TAT) complex levels were assayed using a high-throughput enzyme-linked immunosorbent assay, employing a novel single chain antithrombin-III antibody Nb1024 (Synapse Research Institute). Similarly, as average thrombin lifetimes, 60-minute increases in TAT concentrations (nM) were measured in TF-triggered plasmas.

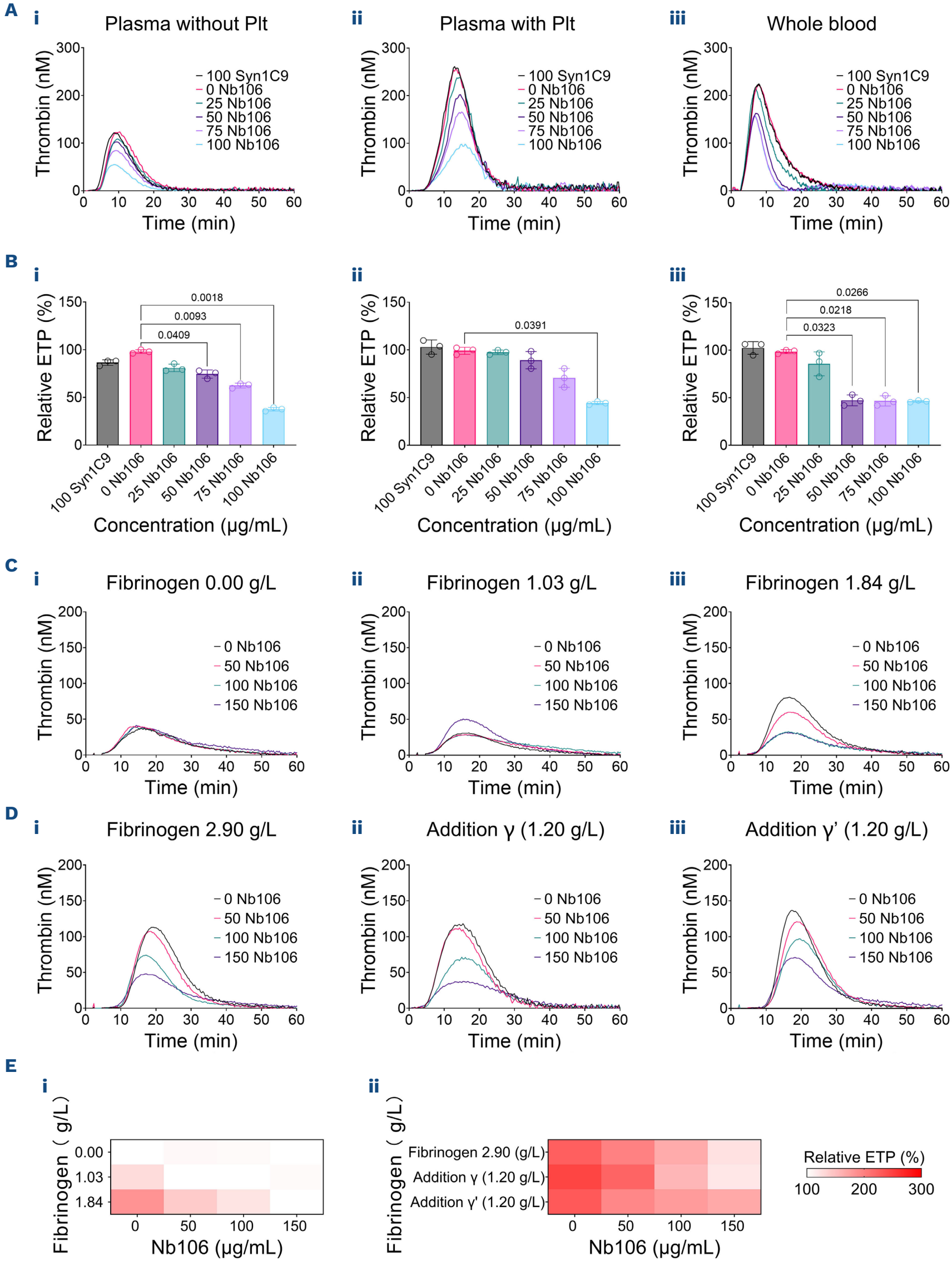

Figure 1. Major anticoagulant effect of fibrin-directed single chain antibody Nb106. (A, B) Samples of plasma, platelet-rich plasma (PRP) and whole blood were preincubated with vehicle control solution, anti-fibrin single chain antibody Nb106 (25-100 μg/

Continued on following page.

mL) or indifferent single chain antibody Syn1C9 (100 μg/mL). Coagulation was triggered with 1 pM tissue factor (TF), phospholipids and $CaCl_2$/$MgCl_2$; see methods. (A) Representative thrombin generation curves with autologous plasma (i), PRP (ii) and whole blood (iii). (B) Quantified thrombin cleavage capacity (endogenous thrombin potential [ETP]), relative to the control condition. Means ± standard deviation (SD) (N=3 experiments). Statistically significant *P* values are shown in the figure (one-way ANOVA, non-parametric). Other parameters indicated in *Online Supplementary Figure S2*. (C, D) Effect of Nb106 in dependency of fibrinogen concentration. (C) Normal pool plasma (NPP, 2.90 g/L fibrinogen) was mixed with fibrinogen-deficient plasma at different volume ratios, and thrombin generation was measured in the presence of 0-150 μg/mL Nb106. Representative thrombin generation is shown (i-iii). (D) NPP was supplemented with fibrinogen-g or fibrinogen-g' (1.2 g/L) and thrombin generation was measured in the presence of of 0-150 μg/mL Nb106. Representative curves given (i-iii). (E i) Heatmap of normalized thrombin capacity for condition of panel C; (E ii) similar heatmap for condition of panel (D). Means ± SD (N=3); 100% represents condition without fibrinogen and Nb106. Plt: platelets; min: minutes.

Results

Potent thrombin-suppressive effect of novel single chain antibody

As a novel approach for investigating the interaction between fibrin and thrombin, we used the single chain antibody Nb106. This antibody was obtained from a llama immunized with human fibrin degradation products, and a constructed VHH library. Antibody selection experiments resulted in Nb106, as a single chain antibody that selectively binds to fibrin but not fibrinogen or thrombin (*Online Supplementary Figure S1A-E*). It appeared to require fibrinopeptide B (FpB) cleavage for recognition, indicating that it targets an epitope associated with the Bβ knob-hole interaction. We concluded that Nb106 recognizes a conformationally exposed site on the β-chain of fibrin that becomes available upon FpB release. Further characterization measurements indicated that Nb106 reduced the binding of thrombin to immobilized fibrin layers (*Online Supplementary Figure S1F, G*).

Investigating the TF-triggered coagulation process, we observed a profound suppressive effect of Nb106 on maximal thrombin levels and thrombin-cleaving capacity (area-under-the-curve, aka ETP) in platelet-poor plasma, in PRP and whole blood (Figure 1A, B). For the thrombin generation process, we observed a dose-dependent inhibition, up to 50% at saturating concentration of 7.5 mM Nb106 (100 μg/mL), i.e., far below the normal fibrinogen concentration of 2-4 mg/mL. The indifferent single chain antibody Syn1C6 was ineffective. Although Nb106 caused a major reduction in thrombin level, it did not alter the generation kinetics (*Online Supplementary Figure S2A, B*), suggesting interference in a post-acute phase of the clotting process.

To study the contribution of the fibrinogen level, we mixed fibrinogen-depleted plasma and normal plasma in various ratios, and re-assessed the TF-triggered coagulation process. Without fibrinogen, relatively low amounts of thrombin were formed that were not sensitive to Nb106 (150 μg/mL). At higher fibrinogen concentrations, both the thrombin level and the suppression by Nb106 increased (Figure 1C). Addition of g'-enriched fibrinogen to normal plasma resulted in a reduced Nb106 effect, compared to normal fibrinogen (Figure 1D, E). This suggested that Nb106 did not interfere with the high-affinity binding site for thrombin in fibrinogen-g'.[14] When Nb106 was spiked into normal plasma at later time points, the inhibitory effect disappeared after 5-10 minutes of TF triggering (*Online Supplementary Figure S2C, D*). Hence the time slot of suppression coincided with the build-up of the fibrin clot.

To assess the reliance on coagulation factors, we studied thrombin generation in several coagulation factor-deficient plasmas. We observed that Nb106 caused major reductions in thrombin formation in normal pool plasma (NPP) and in plasmas deficient in coagulation factors IX, XI or XII (Figure 2A-D). In contrast, it was ineffective in the absence of fibrinogen or antithrombin-III (Figure 2E, F), as quantified from measured thrombin maxima and thrombin capacity levels (Figure 2G). This requirement of fibrinogen and antithrombin was also retained in the presence of platelets (*Online Supplementary Figure S3A-G*). As expected, at antithrombin-III deficiency, higher thrombin levels were reached, with maxima raising from 150 to 450 nM (Figure 2F), due to the impaired inactivation of proteolytically active thrombin.

To determine whether the fibrinogen dependence was pertained upon triggering of the intrinsic pathway, we measured the kaolin-induced thrombin generation. Similar to the TF-triggered condition, Nb106 reduced the thrombin capacity by 57.39±21.79 % in NPP, but not in fibrinogen-deficient plasma (*Online Supplementary Figure S4A-C*).

Assessment of the fibrin-bound pool of active thrombin attacked by Nb106

From the results so far, we hypothesized that the Nb106 displaces thrombin from growing fibrin fibers, thereby rendering it susceptible to inhibition by antithrombin-III through TAT complex formation. To check this, we measured average thrombin lifetimes in both normal and antithrombin-deficient plasma, i.e., by comparing the thrombin capacity (ETP, nM x min) and the prothrombin consumption (nM) after 60-minutes of TF triggering (Figure 2H, I). Herein, we distinguished between a fibrin-independent thrombin pool 1 (thrombin capacity resistant to Nb106), and a fibrin-dependent thrombin pool 2 for the remaining capacity (Figure 2J). Using NPP, average thrombin lifetimes for pool 1 and 2 were obtained of 1.21±0.13 and 2.70±0.45 minutes, respectively (means ± standard deviation [SD], N=5). For antithrombin-deficient plasma

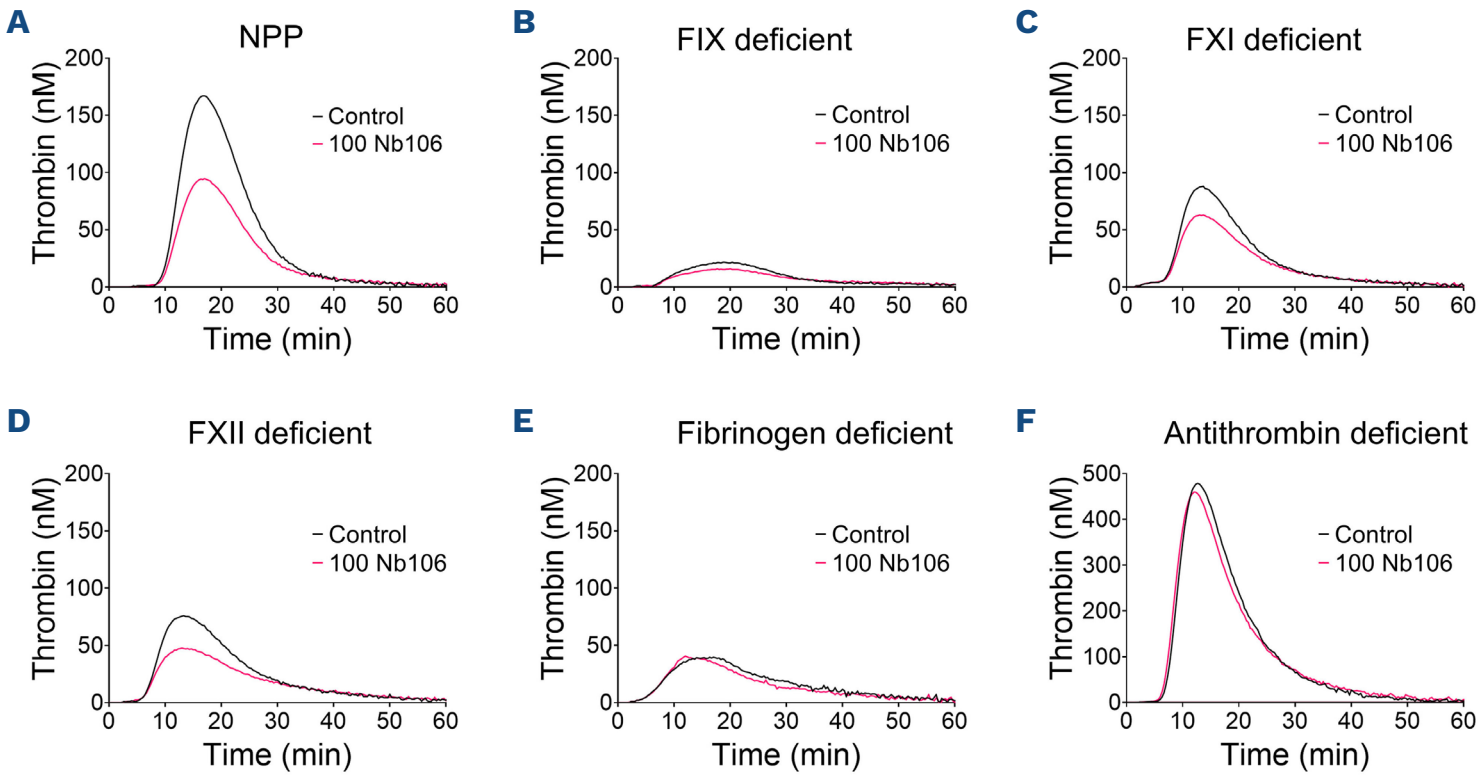

G

Factor deficiency	Effect of Nb106 (control 100%)					
	Relative lagtime (%)	*P*	Relative peak (%)	*P*	Relative ETP (%)	*P*
None (NPP)	104 ± 3	0.12	57 ± 8	0.003	62 ± 8	0.002
Fibrinogen	102 ± 3	0.37	102 ± 19	0.96	89± 11	0.20
Factor IX	104 ± 3	0.10	73 ± 4	0.004	85 ± 6	0.01
Factor XI	103 ± 2	0.12	72 ± 2	< 0.001	80 ± 1	< 0.001
Factor XII	102 ± 6	0.64	63 ± 4	0.001	75 ± 2	0.001
Antithrombin	95 ± 0.1	0.10	92 ± 4	0.12	97 ± 1	0.20

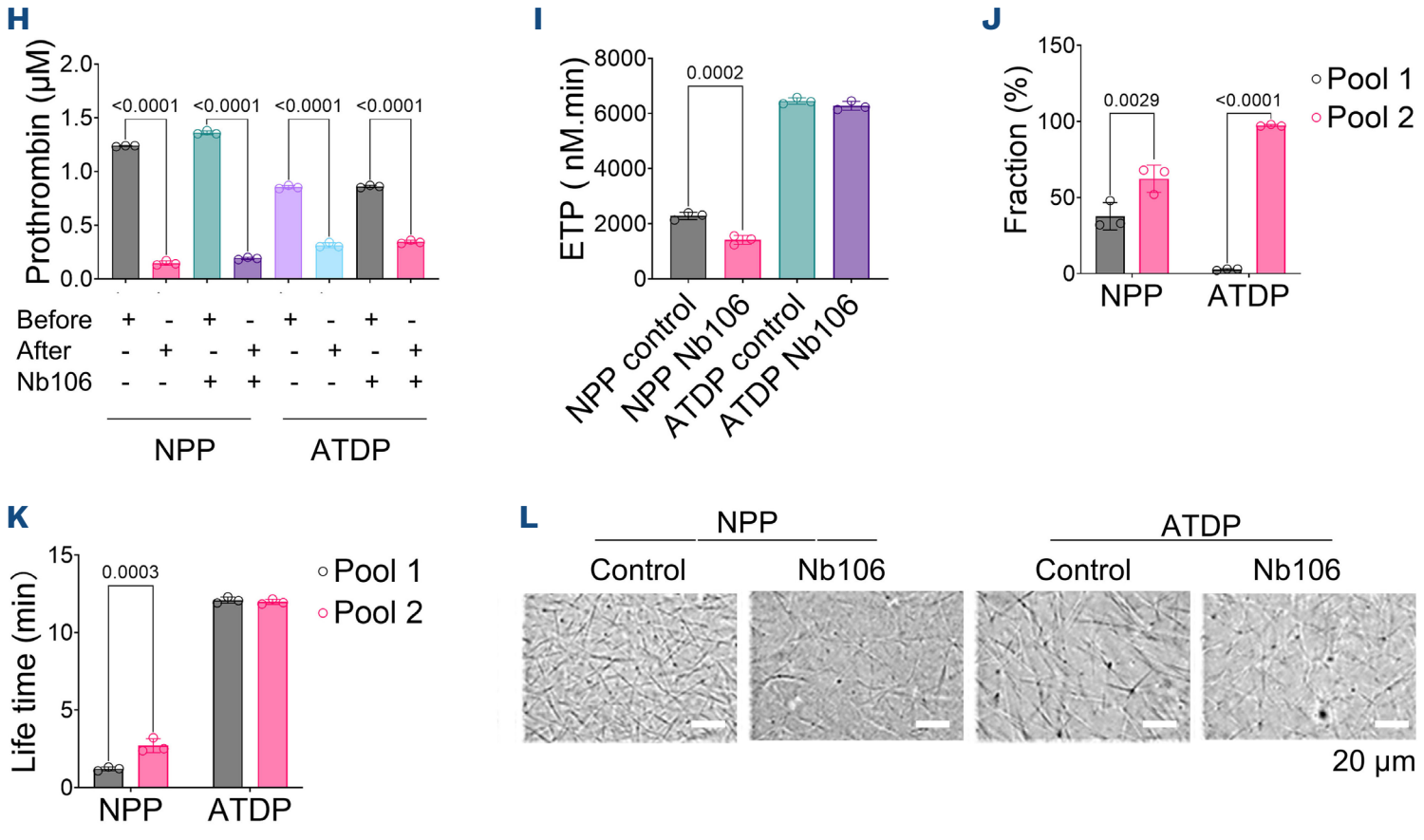

Figure 2. Anticoagulant effect of Nb106 relying on both fibrinogen and antithrombin. (A-G) Tissue factor (TF)-triggered thrombin generation was measured in different plasma types containing vehicle control solution or Nb106 (100 μg/mL), as in Figure 1. Compared were normal pool plasma (NPP) (A), and plasmas deficient in factor IX (B), factor XI (C), factor XII (D), fibrinogen (E), or antithrombin (F). Generation of thrombin over time (N=3) and process quantification with statistics (G). (H, K) Assessment of fibrin-independent and -dependent thrombin pools 1 and 2 in coagulating plasma. NPP and antithrombin-deficient plasma (ATDP) were activated as above, and thrombin capacity (endogenous thrombin potential [ETP]) measured over 60 minutes (min). (H). Prothrombin consumption over 60 minutes assessed in activated subsamples (I). Fractions (J) and lifetimes (K) of thrombin pool

Continued on following page.

1 (Nb106-insensitive, fibrin-independent in NPP) and pool 2 (Nb106-sensitive, fibrin-dependent in NPP) were calculated, as in the methods section. Means ± standard deviation (SD) (N=3-5), two-way ANOVA, non-parametric. (L) Fibrin fiber structures formed in NPP and antithrombin-deficient plasma. Human NPP and antithrombin-III-deficient plasma (ATDP) was triggered with TF, pro-coagulant phospholipids and Ca^{2+}. Plasma samples were preincubated with vehicle control medium or Nb106 (100 μg/mL). Shown are representative brightfield microscopic images (bar=20 μm) from triplicate experiments.

(no Nb106 effect) this lifetime was prolonged to 11.98±0.17 minutes (Figure 2K). These values are in line with literature where thrombin was spiked into antithrombin-deficient plasmas.[22] Hence, we concluded that the fibrin-binding Nb106 shortened the average thrombin lifetime by 2.2-fold, whereas the absence of antithrombin-III prolonged this lifetime by 9.9-fold.

Initial light transmission microscopy indicated that Nb106, in both TF-triggered NPP and antithrombin-deficient plasma, made the fibrin fiber network less compact (Figure 2L). Fibrin fibres also appeared thicker without antithrombin-III. This suggested that, in normal plasma, the fibrin-bound (Nb106-replacable) pool of thrombin has a critical role in fibrin network formation.

Considering prior evidence of a thrombin binding site in N-terminal regions of fibrin Aα and Bβ chains,[13] we assessed how Nb106 acted in plasmas pretreated with specific fibrinogen-cleaving proteases. Plasma incubation with protease III from the snake Crotalus atrox, which N-terminally cleaves fibrinogen Bβ-chains,[23,24] halved the thrombin generation and importantly annulled the inhibition by Nb106 (*Online Supplementary Figure S5A*). Plasma treatment with ancrod from *Calloselasma rhodostoma*, which C-terminally cleaves fibrinogen Aa-chains,[25] was however ineffective on coagulation in the presence or absence of Nb106 (*Online Supplementary Figure S5B*). Addition of the fibrin polymerization-inhibiting peptide GPRP[26] reduced thrombin generation by 20%, but did not alter the suppression by Nb106 (*Online Supplementary Figure S5C*).

We then checked for effects with clinically relevant anticoagulants, using the reversible thrombin inhibitor dabigatran or activated protein C. Although either intervention suppressed thrombin generation as expected, both left the extent of Nb106 inhibition unchanged (*Online Supplementary Figure S5D, E*). To substantiate the idea that Nb106 displaces thrombin from growing fibrin fibers, we first examined the effects of the irreversible thrombin inhibitor PPACK. This treatment caused a concentration-dependent delay and reduction in thrombin generation, whereas the inhibitory effect of Nb106 remained unchanged (*Online Supplementary Figure S7A*). Second, we made a purified preparation of PPACK-inactivated thrombin, blocking its active site but retaining the exosites (*Online Supplementary Figure S6*). Strikingly, the addition of PPACK-thrombin to NPP suppressed the thrombin generation to the same extent as Nb106 (*Online Supplementary Figure S7B*). In contrast, the PPACK-thrombin was without effect in fibrinogen-deficient plasma (*Online Supplementary Figure S7C*). These results suggested that both NB106 and PPACK-thrombin compete with active thrombin for binding sites on fibrin, and thereby promote inactivation of the released thrombin by antithrombin-III. Additionally, these findings provide an indication that the Nb106 binding site in fibrin locates near the N-terminal Bb chain in the D-E-D domain, i.e., a known fibrin knob-allocated position of thrombin.[13] We hence concluded that displacement of thrombin in the E domain can relieve its protection to antithrombin-III inactivation.

Inter-subject variability of thrombin generation not affected by Nb106

To assess for inter-subject differences, we also assessed the TF-triggered coagulation in plasmas from 64 healthy subjects, applying a near maximal inhibiting Nb106 concentration of 150 μg/mL. Across all subjects, Nb106 did not alter thrombin lag times, while it consistently reduced thrombin maxima and thrombin capacity levels by 53±11% and 55±12% (mean ± SD, N=64; $P<0.05$), respectively (*Online Supplementary Figure S8A, B*). Interestingly, when plotted against the fibrinogen activity level (Claus method), we noticed an increased capacity, which was corrected by the Nb106 up to 4 g/L fibrinogen. This demonstrated a consistent downregulation of thrombin generation by the antibody. However, thrombin capacities with and without Nb106 were strongly correlated ($R^2=0.66$; $P<0.0001$) (*Online Supplementary Figure S8D*). Across plasmas, the extent of thrombin capacity inhibition by Nb106 showed a statistically significant but modest correlation ($R^2=0.15$; $P=0.0019$) (*Online Supplementary Figure S8C*), in support of crucial roles of other coagulation factors in the thrombin generation process.[27,28]

Displacement of thrombin from fibrin altering fibrin fiber structure and function

Considering the potent antithrombin effect of Nb106, we next examined how it affected fibrin protofibril formation and polymerization. In measurements of mechanically stirred clotting times, plasma triggering with 1-1,000 pM TF was not affected by Nb106 (Figure 3A). In contrast, in light disturbance measurements, Nb106 essentially annulled the TF-induced optical density changes (Figure 3B). This suggested that the clots formed with Nb106 are light transparent, which idea was also supported by confocal microscopy, showing fibrin microclots not extending to fibrin fibers (*Online Supplementary Figure S9A*). Additional clot lysis experiments showed that the loose transparent clots formed with Nb106 were still susceptible to tPA-induced lysis, although the minimal turbidity changes preclude reli-

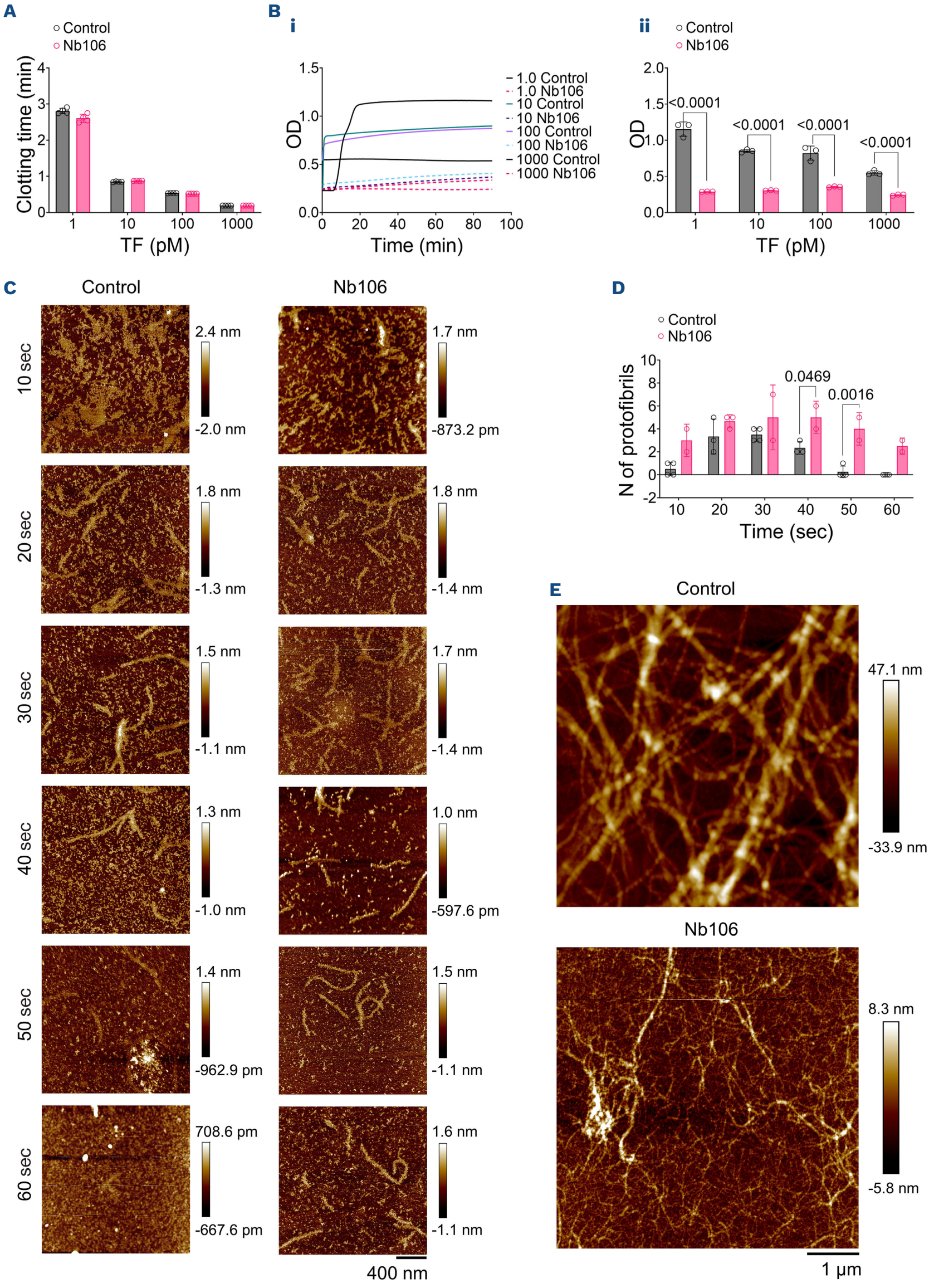

Continued on following page.

Figure 3. Displacement of thrombin by Nb106 profoundly altering fibrin fiber structures but not clotting as such. (A, B) Human plasma containing vehicle control medium or Nb106 (100 μg/mL) was triggered with tissue factor (TF) (1-1,000 pM), phospholipids and $CaCl_2$. (A) Effect of Nb106 on TF-induced mechanical (stirred) clotting time. (B) Abrogated TF-induced turbidity changes in coagulating plasma with Nb106 over time (i), plus quantification after 80 minutes (ii). Means ± standard deviation (SD) (N=3-4 experiments, two-way ANOVA, non-parametric). (C-E) Atomic force microscopy (AFM) was employed for imaging of the fibrin protofibril assembly in preparations of human fibrinogen (0.5 mg/mL), $CaCl_2$ (2.5 mM) and thrombin (10 nM) in Tris-buffered saline, allowed to react for 10-60 seconds (sec) or 5 minutes (min). Control vehicle or Nb106 (100 mg/mL) was added to the mixtures as indicated. Prepared samples on mica discs were examined with a Nanoscope IIIa MultiMode microscope operating in tapping mode. (D) Shown are representative images of fibrinogen, protofibril and polymerized fibrin molecules. Blue arrows indicate single molecule fibrin protofibrils. (E) Numbers of protofibrils per image of 2 x 2 mm. Mean ± SD (N=3-4, two-way ANOVA multiple comparison test). (F) End stage images after 5 minutes of fibrinogen cleavage. Note major reduction in size and length of fibrin fibers formed in the presence of Nb106. OD: optical density.

able determination of the lysis time (*Online Supplementary Figure S9B*).

Fibrin fiber formation proceeds by polymerization of fibrin monomers into protofibrils.[19] For higher-resolution examination, we applied atomic force microscopy allowing visualization of the protofibril formation on a molecular scale. Using mixtures of fibrinogen and thrombin, we observed that the Nb106 within 1 minute enhanced and retained the formation of protofibril molecules (Figure 3C, D). This effect is compatible with thrombin displacement from the central D-E-D regions, which results in more soluble thrombin to induce additional fibrinogen cleavages. Longer-time images showed that Nb106 blocked normal extension of fibrin fibers, leaving shorter and thinner protofibril structures (Figure 3E). These profound structural changes prompted us to examine Nb106 effects on the physiological and biophysical properties of formed clots under conditions of dysfibrinogenemia.

Altered thrombin generation and fibrin clots in patients with congenital dysfibrinogenemia

Patients with congenital dysfibrinogenemia exhibit functional alterations in fibrinogen, which are asymptomatic or associate with bleeding or thrombotic events.[29] Multiple pathogenic mutations have been identified, in part dominant, which concentrate in distinct regions of the *FGA*, *FGB* and *FGG* genes.[9,30] To examine the thrombin-fibrin interactions in dysfibrinogenemia, we studied plasmas from 21 patients with a mutation in *FGA* (N=12), *FGB* (N=4) or *FGG* (N=5). Given the rarity of this disorder, this cohort represents one of the largest collections of patients with fibrinogen gene mutations.

All patients presented with a low fibrinogen function (assessed by the Claus method) relative to the fibrinogen antigen level, while 11 patients had sub-normal antigen levels as well (Table 1). Across mutations, nine patients had experienced minor bleeding symptoms, two had thrombotic events, while for three mutations (9 additional patients) incidental bleeding and thrombosis has been documented (Table 1). With all patients showing lower fibrinogen function than antigen levels, they were analyzed as a single group, despite the heterogeneity in mutation type and gene and clinical penetrance.

Coagulation analysis indicated that in plasmas from 13 of 21 patients, across all three genes, thrombin generation exceeded the reference values assessed for healthy subjects, while only three plasmas showed low maximal thrombin levels (<150 nM) (Table 1). Addition of Nb106 suppressed both the maximal and capacity levels, whilst values remained supranormal in 11-14 patients (Figure 4A-F). Lowest suppression of <40% was observed in the six patients with sub-normal functional fibrinogen, i.e., 0.77±0.43 g/L (mean ± SD). When plotted against the fibrinogen function level, the patient group as a whole scored high in thrombin generation (Figure 4G). This could be considered as clinically relevant, since already small increases in thrombin generation profiles have been associated with thrombogenic abnormalities.[31,32] Six of the patients (3x *FGA*, 2x *FGB*, 1x *FGG* mutations) with high thrombin generation had experienced bleeding symptoms (Table 1).

In the patient group, TF-triggered clot retraction in the presence of platelets was high given taking into account their low fibrinogen values (Figure 4H), but this was not the case for plasma turbidity changes (Figure 4I). Together, this suggested an enhanced activity of fibrin-bound (anti-thrombin-resistant) thrombin, yet showing high contractility, in at least part of the patient plasmas. To further assess this, we measured the complex formation of thrombin-antithrombin (TAT) in activated plasma samples from controls and patients, using a new single chain antibody Nb1024. Since TAT levels reflect prothrombin consumption when combined with thrombin capacity values, these were also used to calculate average thrombin lifetimes. Markedly, we observed significantly lower TAT levels in the total patient group, when compared to the controls, which translated into prolonged thrombin lifetimes for half of the patients (Figure 4J-K). These results jointly show that, in at least part of the studied dysfibrinogenemia patients, across gene mutations, the altered fibrinogen function is accompanied by a prolonged activity of fibrin-bound thrombin. The combination of loss-of-function (low or dysfunctional fibrinogen) and gain-of-function (enhanced thrombin activity) may underlie the paradoxical coexistence of hemostasis and thrombotic complications regularly observed in these patients.

Table 1. Characteristics of plasmas from patients with congenital dysfibrinogenemia.

Patient	Genetic variant	Sex	Age, years	Patient phenotype	Mutation-linked phenotype in literature	Fibrinogen antigen g/L	Fibrinogen function g/L	Thrombin maximum nM
FGA1	FGA c.95 G>A (p.Gly32Glu) het	M	28	prolonged PT	likely pathogenic	2.64	1.06*	678#
FGA2	FGA c.95 G>A (p.Gly32Glu) het	M	62	epistaxis in childhood	likely pathogenic	3.03	1.08*	504#
FGA3	FGA c.112 A>G (p.Arg38Gly) het	M	53	prolonged PT	reported bleeding and thrombosis, polymer region	3.03	0.65*	328#
FGA4	FGA c.149 C>G (p.Ser50*) hom	F	61	cranial bleeding, aortic thrombosis	novel (ND)	1.30*	0.35*	320#
FGA5	FGA c.112 A>G (p.Arg38Gly) het, FGB c.794 C>T (p.Pro265Leu) het	F	63	family study	reported bleeding and thrombosis, polymer region (FGA)	3.18	1.04*	202
FGA6	FGA c.112 A>G (p.Arg38Gly) het	F	22	prior bleeding	reported bleeding and thrombosis, polymer region	2.40	0.58*	297#
FGA7	FGA c.104 G>A (p.Arg35His) het	M	23	asymptomatic	reported bleeding and thrombosis (pathogenic)	3.17	1.40*	174
FGA8	FGA c.104 G>A (p.Arg35His) het	F	39	mild bleeding	reported bleeding and thrombosis (pathogenic)	2.70	1.30*	236
FGA9	FGA c.104 G>A (p.Arg35His) het	F	38	mild bleeding	reported bleeding and thrombosis (pathogenic)	3.26	1.40*	387#
FGA10	FGA c.104 G>A (p.Arg35His) het	F	27	mild bleeding	reported bleeding and thrombosis (pathogenic)	2.19*	1.10*	158
FGA11	FGA c.104 G>A (p.Arg35His) het	M	39	asymptomatic	reported bleeding and thrombosis (pathogenic)	3.54	1.50	233
FGA12	FGA c.104 G>A (p.Arg35His) het	F	22	asymptomatic	reported bleeding and thrombosis (pathogenic)	2.18*	0.60*	275#
FGB1	FGB c.886 T>C (p.Trp296Arg) hom	M	5	prior bleeding	novel (ND)	1.11*	0.68*	329#
FGB2	FGB c.886 T>C (p.Trp296Arg) het	M	38	bleeding after minor injuries	novel (ND)	1.38*	1.06*	531#
FGB3	FGB c.886 T>C (p.Trp296Arg) het	F	26	family study	novel (ND)	1.71*	1.09*	559#
FGB4	FGB c.534 G>C (p.Lys178Asn) het	M	28	family study	novel (ND)	1.98*	1.61	141
FGG1	FGG c.998 A>G (p.His333Arg) het	M	44	thrombosis of superior mesenteric vein	novel (ND)	0.84*	0.42*	386#
FGG2	FGG c.998 A>G (p.His333Arg) het	F	13	prior bleeding	novel (ND)	1.14*	0.91*	271#
FGG3	FGG c.1223 C>T (p.Thr408Ile) het	M	24	prolonged PT	novel (ND)	0.87*	0.85*	276#
FGG4	FGG c.323 C>G (p.Ala108Gly) het	M	41	prior bleeding	reported bleeding (likely pathogenic)	1.74*	1.60	114
FGG5	FGG c.1007 T>C (p.Met336Thr) het	F	27	menorrhagia prolonged PT	fibrinogen Asahi (pathogenic)	4.26	0.35*	99
Ref. values	-	-	-	-	-	2.4-3.6	1.5-4.5	80-254

Values below the normal range are marked with *, and those above are marked with #. F: female; M: male; ND: not defined; het: heterozygous; Ref: reference; PT: prothrombin time. Shown are genetic variants and levels of fibrinogen antigen and function (Claus methods). Reference values for fibrinogen antigen were 2.4-3.6 g/L, for fibrinogen function 1.5-4.5 g/L; and for thrombin generation maxima 80-254 nM. Information on mutation-linked phenotypes came from Ref.[9] and ClinVar Febr. 2025 (https://www.ncbi.nlm.nih.gov/clinvar/). Patients were included, based on studies described before.[16,43]

Thrombin-fibrin interactions affecting thrombus formation at low shear rates

Alignment of the N-terminal regions of fibrinogen Aα- and Bβ-chains showed high amino acid sequence similarly between human and mouse, in particular around the thrombin cleavage site and the adjacent thrombin exosite-I binding domain (*Online Supplementary Figure S10A-D*). The inter-species conservation prompted us to also evaluate the effects of Nb106 in mouse blood. Similar as in the human system, in plasmas from C57BL/6 mice the antibody about halved the maximal thrombin and thrombin capacity levels (Figure 6A), while it similarly distorted the formation of laterally extending fibrin fibers, changing these into amorphous structures (Figure 6B).

As a proxy measurement for thrombus formation *in vivo*, we used a microfluidic approach, in which recalcified whole blood in the presence of TF was flowed over collagen.[21] In this *ex vivo* system, addition of Nb106 (100 mg/mL) led to a significantly reduced and delayed fibrin fiber formation, but unchanged platelet-related thrombus characteristics, upon perfusion of the blood at low, venous wall-shear rate of 200 s^{-1} (Figure 6C-F). On the other hand, upon flow at high arterial shear rate (1,000 s^{-1}), fibrin formation and platelet deposition remained unaltered with Nb106 (*Online Supplementary Figure S11*). Similarly observations were made with human blood (*Online Supplementary Figure S12*). These data point to an overall anticoagulant effect of Nb106 especially under circumstances of stasis or low shear.

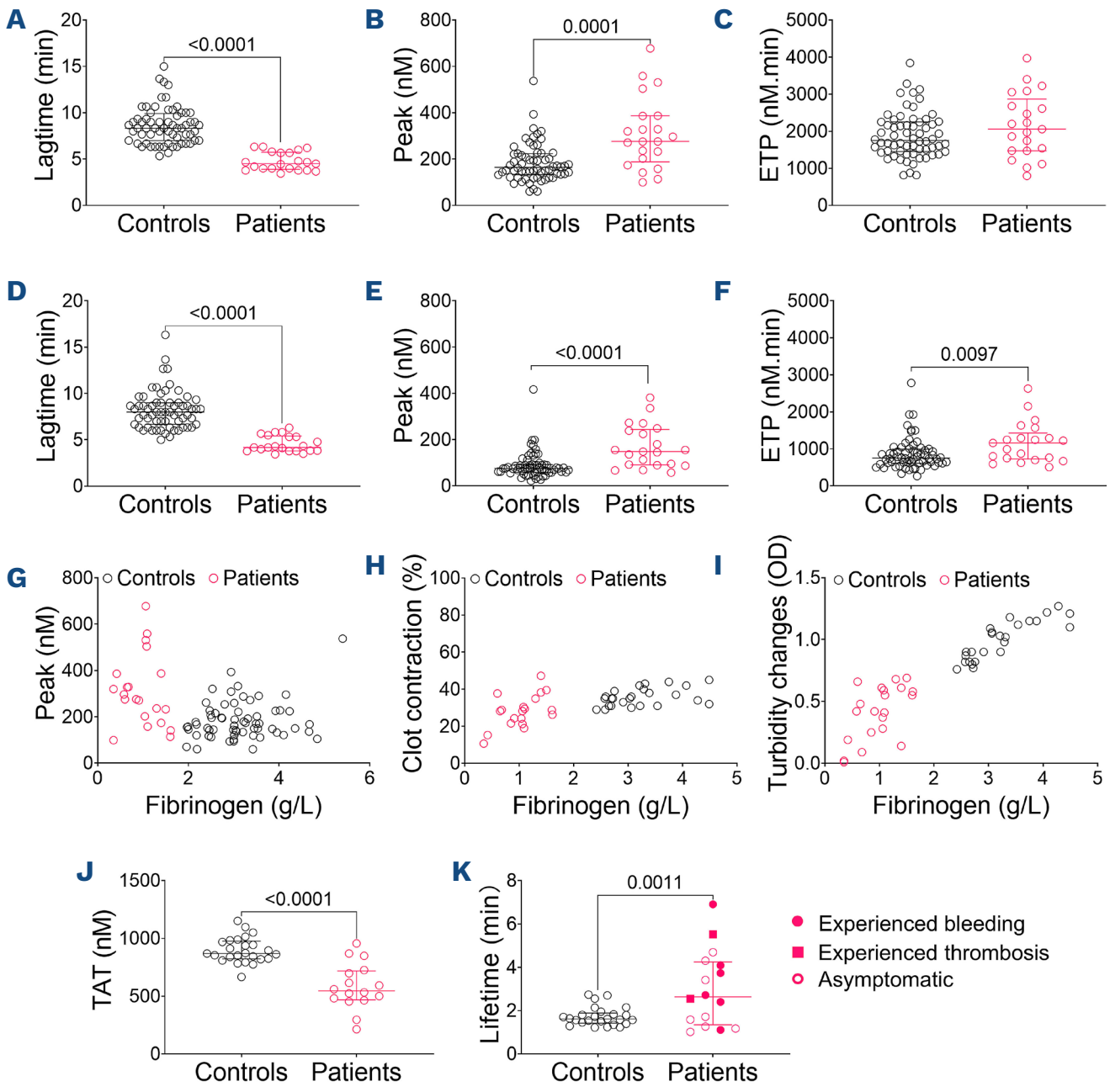

Figure 4. Thrombogenic plasma profile in patients with congenital dysfibrinogenemia. Thrombin generation was compared in plasma samples from 21 patients with congenital dysfibrinogenemia (Table 1) and matching cohorts of healthy subjects (see *Online Supplementary Figure S5*), employing the same trigger conditions (1 pM tissue factor [TF], procoagulant phospholipids, $CaCl_2$), equipment and data processing. Plasmas were in part preincubated with Nb106 (150 μg/mL). (A-F) Comparative thrombin lag times (A, D), maximal thrombin (D, E) and thrombin capacities (C, F) in the absence or presence of Nb106. Medians and interquartile range (N=64 controls, Mann-Whitney U-test). (G-I) Plasmas from 21 patients and 25 healthy subjects were assessed for fibrinogen activity levels (Claus method), and for TF-triggered optical density changes or clot contraction with platelets from a healthy donor. Shown are scatter plots of thrombin capacity (G), clot contraction (platelet count 200×10^9/L), (H), and turbidity changes (I), as a function of the fibrinogen level (patients in red, healthy subjects in black), for control samples. (J, K) Measured thrombin-antithrombin-III (TAT) complexes and active thrombin lifetimes of TF-triggered (60 minutes) individual control and patient samples (non-parametric Mann-Whitney U test). ETP: endogenous thrombin potential; OD: optical density; min: minutes.

Procoagulant effect of fibrin regions interacting with thrombin via exosite I

To further proof the concluded interaction of thrombin with fibrin Aα and/or Bβ N-terminal regions, we synthesized peptides corresponding to the conserved exosite-I binding sites in these regions, i.e., Pep1 consisting of residues 40-69 of fibrinogen-α, and Pep2 composed of residues 71-105 of fibrinogen-β (*Online Supplementary Figure S10*). When tested at 0 and 500 mM, Pep1 but not Pep2 showed a strong but temporary enhancing effect in TF-triggered

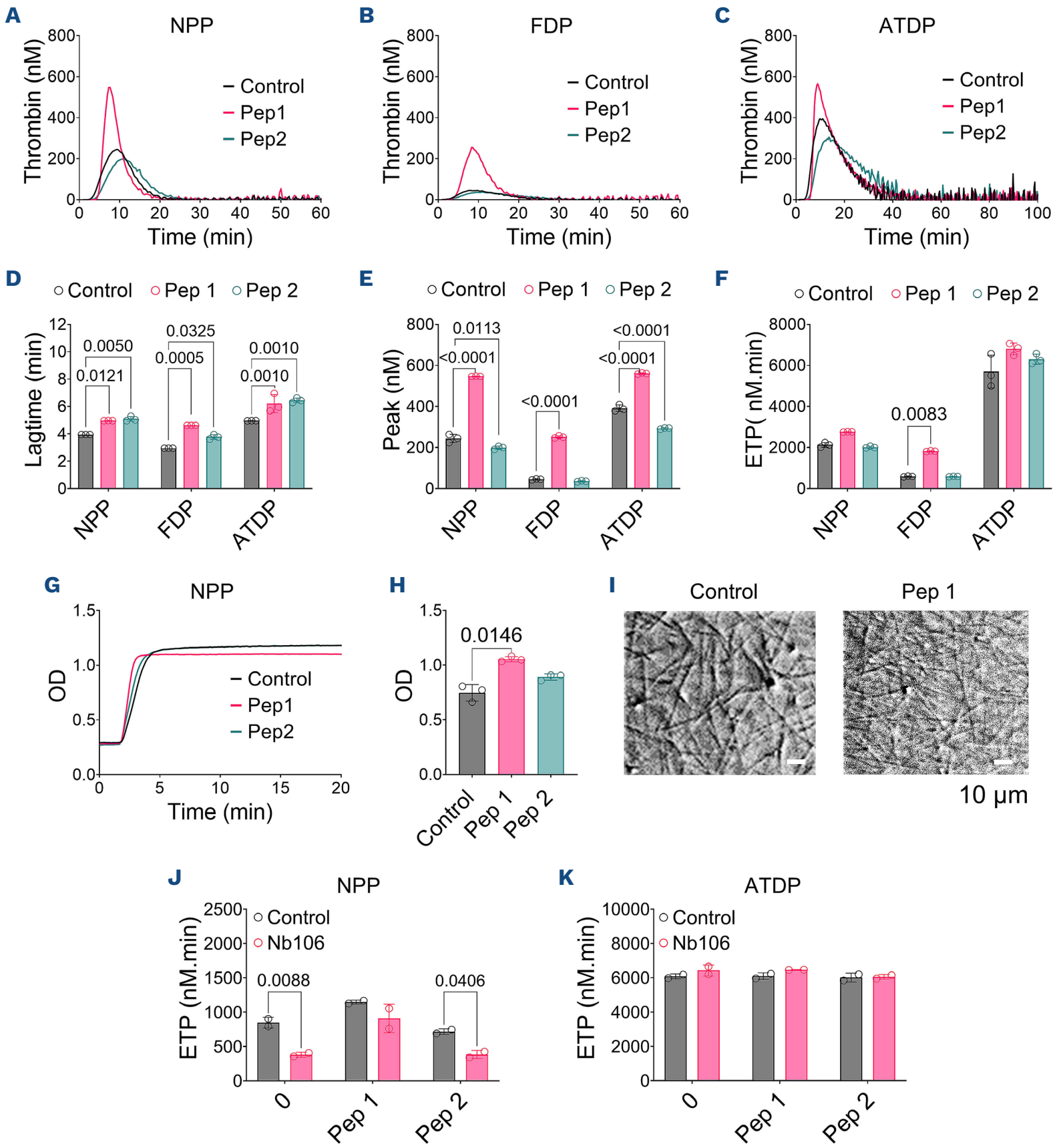

Figure 5. Thrombin-enhancing effect of fibrin-derived synthetic peptides. Functional analysis of synthesized peptide Pep1 consisting of residues 40-69 of fibrinogen-α and peptide Pep2 composed of residues 71-105 of fibrinogen-β (*Online Supplementary Figure S7*). (A-F) Thrombin generation assessed in normal pool plasma (NPP), fibrinogen-deficient plasma and antithrombin-III-deficient plasma (ATDP), measured with 500 µM peptide or vehicle medium after triggering with 1 pM tissue factor (TF). Shown are representative traces (A-C) and quantified lagtime (D) maximal thrombin (E) and thrombin capacity level (F). (G, H) Peptide effects on kinetics of turbidity changes (G) and effect after 3 minutes (H) in normal plasma. (I) Microscopic images of fibrin structure after 20 minutes. (J, K) Combined peptide and Nb106 effects on thrombin capacity in NPP and ATDP, under conditions as in panels (A-F). Mean ± standard deviation (N=3). Statistically significant *P* values are shown in the figure (two-way ANOVA non-parametric). ETP: endogenous thrombin potential; OD: optical density; min: minutes.

thrombin generation at >100 mM, i.e., five-times higher than the bivalent concentration of fibrinogen in normal plasma (Figure 5A). We further found that Pep1 was similarly effective in fibrinogen-depleted and antithrombin-depleted

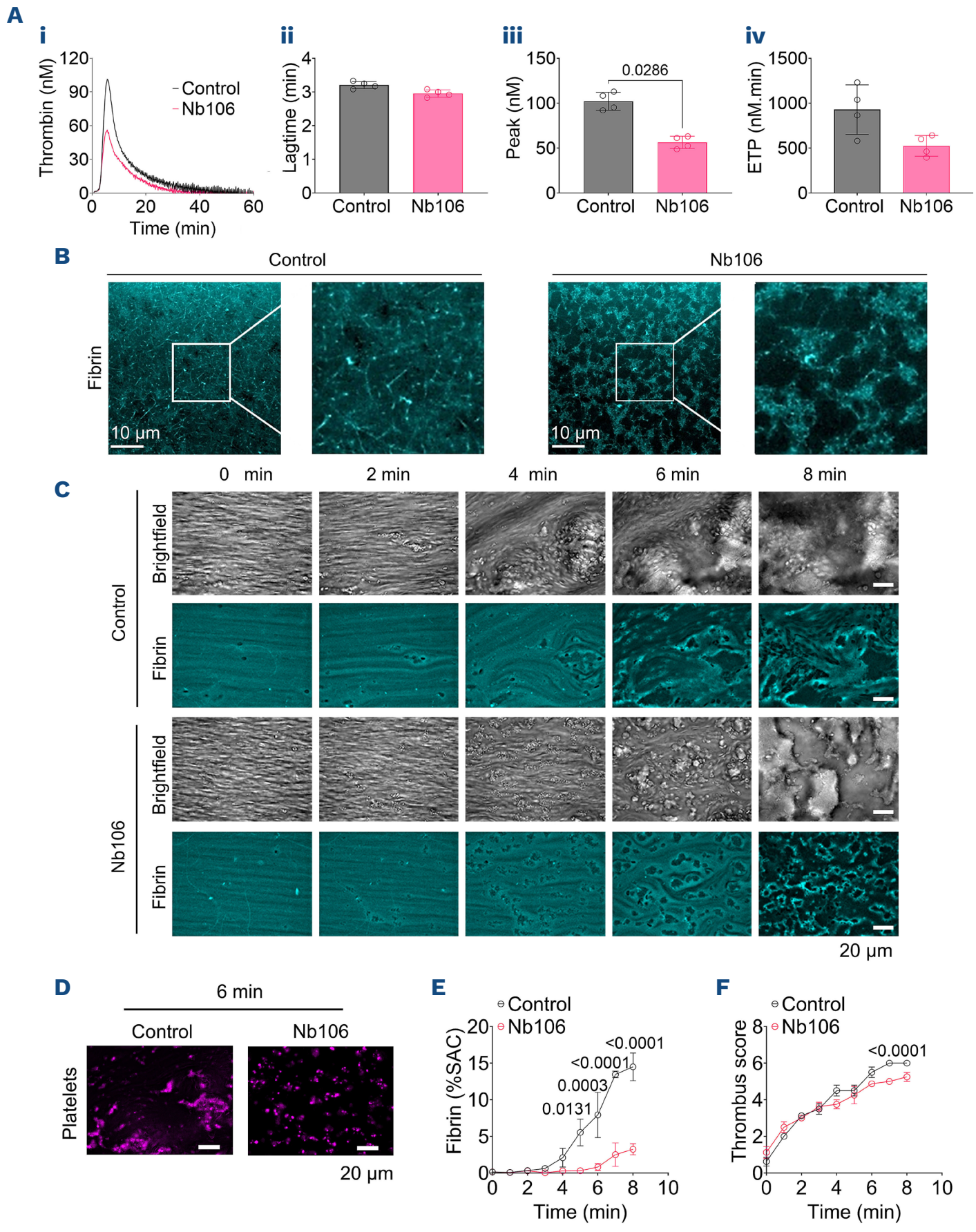

Figure 6. Fibrin-bound thrombin affecting fibrin accumulation in mouse plasma and blood. (A, B) Thrombin inhibiting and fibrin modifying effect of Nb106 in activated mouse plasma. (A) Mouse platelet-rich plasma (PRP) was incubated with vehicle solution or Nb106 (100 μg/mL), and thrombin generation was induced with tissue factor (TF) (1 pM), C-reactive protein (CRP) (10 μg/mL) and $CaCl_2$ (16.6 mM). Shown are representative effects on thrombin generation over time (i), thrombin capacity (endogenous thrombin potential [ETP]) (ii), maximal thrombin level (iii) and thrombin lagtime (iv). Mean ± standard deviation (SD) (N=4), non-parametric Mann-Whitney U test. (B) Mouse plasma containing Alexa Fluor 488-fibrinogen with(out) Nb106 (100 μg/mL) was triggered with 1 pM TF, phospholipids and $CaCl_2$ for confocal microscopic assessment of fibrin formation. Representative images recorded after 100 minutes (min). (C-F) Citrated mouse blood was supplemented with Alexa Fluor 488-fibrinogen (green) and Alexa Fluor 647-anti-GPIX monoclonal antibody (mAb) (purple), with Nb106 (100 μg/mL) present as indicated. (C) Blood samples were continuously recalcified with 1 pM TF, while perfusing over collagen-I microspots at low, venous wall-shear rate of 200 s^{-1}. (D) Representative images of 6-min platelet deposition (AF647-αGPIX). (E, F) Quantification of fibrin surface area coverage and thrombus score on scale 1-6 over time.[20] Mean ± SD (N=4), non-parametric Mann-Whitney U test. OD: optical density.

plasma. In all cases, it caused a transient enhancement in thrombin levels, regardless of the slower decay in the absence of antithrombin-III (Figure 5A-F). In addition, Pep1 but not Pep2 shortened TF-triggered turbidity changes in plasma (Figure 5G, H) and prolonged the clot lysis time (*Online Supplementary Figure S9C*), but it did not appreciably affect fibrin network formation (Figure 5I). Pep1 furthermore reduced the inhibiting effect of Nb106 (Figure 5J, K). Taken together, this suggested that also Pep1, as thrombin exosite-I binding peptide derived from the fibrin Aα N-terminal region, - likely in equilibrium with the corresponding sequence in fibrin - temporarily protected thrombin for inactivation by antithrombin-III.

To confirm this, we tested aptamers directed against thrombin exosite-I (Apt1), exosite-II (Apt2), or both (Apt3). We found that Apt1 and Apt2 similarly enhanced thrombin generation but now leaving the inhibiting effect of Nb106 unaffected (*Online Supplementary Figure S13*). In contrast, Apt3 fully blocked the process, i.e., by effectively annulling thrombin activity (*Online Supplementary Figure S13D, H*). These results jointly indicate that interference in the binding of thrombin to antithrombin-III enhances its cleavage capacity.

Discussion

Our study reveals the key importance of N-terminal regions in the fibrin Aα- and Bβ-chains regarding binding and retaining proteolytically active thrombin to allow lateral extension of fibrin fibers. Mechanistically, we show that this binding provides temporal protection against inactivation by antithrombin-III. This insight and the various tools developed in our study can provide novel approaches to rebalance the fibrin clotting process in (venous) thrombosis and impaired haemostasis.

Insight into the role of thrombin-bound fibrin came from the use of a novel single chain antibody Nb106, raised against fibrin degradation products and characterized as binding to fibrin D-E-D regions, but not to full length fibrinogen. In TF-triggered plasma or blood, Nb106 abrogated half of the thrombin cleavage capacity, which effect relied on the presence of both fibrinogen and antithrombin-III. Supported by experiments using PPACK-thrombin, our data indicated that Nb106 released thrombin from growing fibrin fibres, thereby enhancing its inactivation by antithrombin-III. As the Nb106 effect disappeared after fibrinogen treatment with protease III, we considered that the binding site is at or close to the N-terminal region of fibrin Bβ. Conversely, the peptide Pep1 corresponding to the N-terminal Aa chain increased the thrombin activity, similarly as thrombin exosite-I binding aptamers, which region according to crystallographic evidence locates close to the N-terminal Bb chain. This scheme agrees with the known structure of two thrombin molecules bound to central E-domain of fibrin via exosite-I recognition sites in the Aα and Bβ chains (Figure 7A-D).

Our findings are also in agreement with the early, 1997, identification of low affinity thrombin binding sites on fibrin, which were then provisionally assigned to the N-terminal Aα chains and Bβ chains, i.e., adjacent to the thrombin cleavage sites producing FpA and FpB, respectively. Of note, there is evidence that similar sites are also involved in fibrin monomer polymerization,[23,36] suggesting that also fibrin monomer competition dislodges thrombin from growing fibers, and thereby re-exposes its active site for clot extension.[34] Our measurements of thrombin activity and prothrombin consumption made us conclude that the binding to fibrin led to a 2.2-fold increase in average lifetime, which is less than the 10-fold increase observed in the absence of antithrombin-III.

We furthermore observed that the thrombin binding was required for lateral growth of fibrin monomers to form the network of fibrin fibers. The abrogation of optical density changes in clotting plasma with Nb106, despite unaltered clotting times, could be explained by the formation of transparent, essentially non-fibrillar clots in the presence of Nb106. Also other authors have observed that the formation of a thin fibrin network causes minimal changed in light scattering.[37] Our atomic force microscopy experiments also demonstrated that Nb106 stimulated the formation of thin and amorphous protofibrils instead of mature fibrin fibers. Jointly, our data point to the presence of a substantial pool of proteolytically active thrombin that binds to fibrin, is protected from anticoagulation, and is required for elastic fibrin clot formation.

To further substantiate the findings, we defined and quantified two similarly sized thrombin pools: a fibrin-dependent (Nb106-sensitive) pool, corresponding to the fraction of thrombin capacity suppressed by Nb106, and a fibrin-independent (Nb106-insensitive) pool, corresponding to the remaining capacity unaffected by the antibody. This approach supported the view that fibrin serves as a dynamic reservoir maintaining thrombin activity at the clot interface. Mechanistically, as stipulated for other natural thrombin inhibitors,[38] our data demonstrate that fibrin acts as a potent redirector of thrombin's targets in coagulation. In analogy, endothelial-expressed thrombomodulin redirects thrombin's targets towards protein C activation.[39] The unravelled prolonged binding of thrombin to fibrin further explains earlier *in vivo* observations on thrombotic venules and arterioles in mouse, showing consistent co-localization of labeled (pro)thrombin with formed fibrin clots.[40]

Patients with congenital dysfibrinogenemia carrying variety of mutations in the fibrinogen genes *FGA, FGB* or *FGG*, present with heterozygous symptoms, where a mild bleeding phenotype is more frequently observed than thrombophilia.[9,41] This is also seen in the 21 patients included in the present study, with half of the subjects showing mostly mild bleeding symptoms and two presenting with

thrombotic complications. Intriguingly, the majority of 13 patients showed higher than normal thrombin generation levels, which were partly normalized by Nb106, whereas only three patients had relatively low levels. It should be mentioned here that the molecular relation between the usually heterozygous mutations and the phenotype is complex, because of the presence of heterodimeric fibrinogen molecules.[9]

In the patient group, we furthermore noted a lower than normal TAT complex formation. Comparison of the thrombin generation profile and the TAT formation pointed to a prolonged average thrombin lifetime in the whole patient group. This hence suggests a prolonged retainment of thrombin at the fibrin network, which is in line with the often altered (porous, lace-like, thick fiber) fibrin networks observed in dysfibrinogenemia.[42] Our data with 21 patients however will need to be followed up by more detailed studies to establish the precise relation between a prolonged thrombin activity

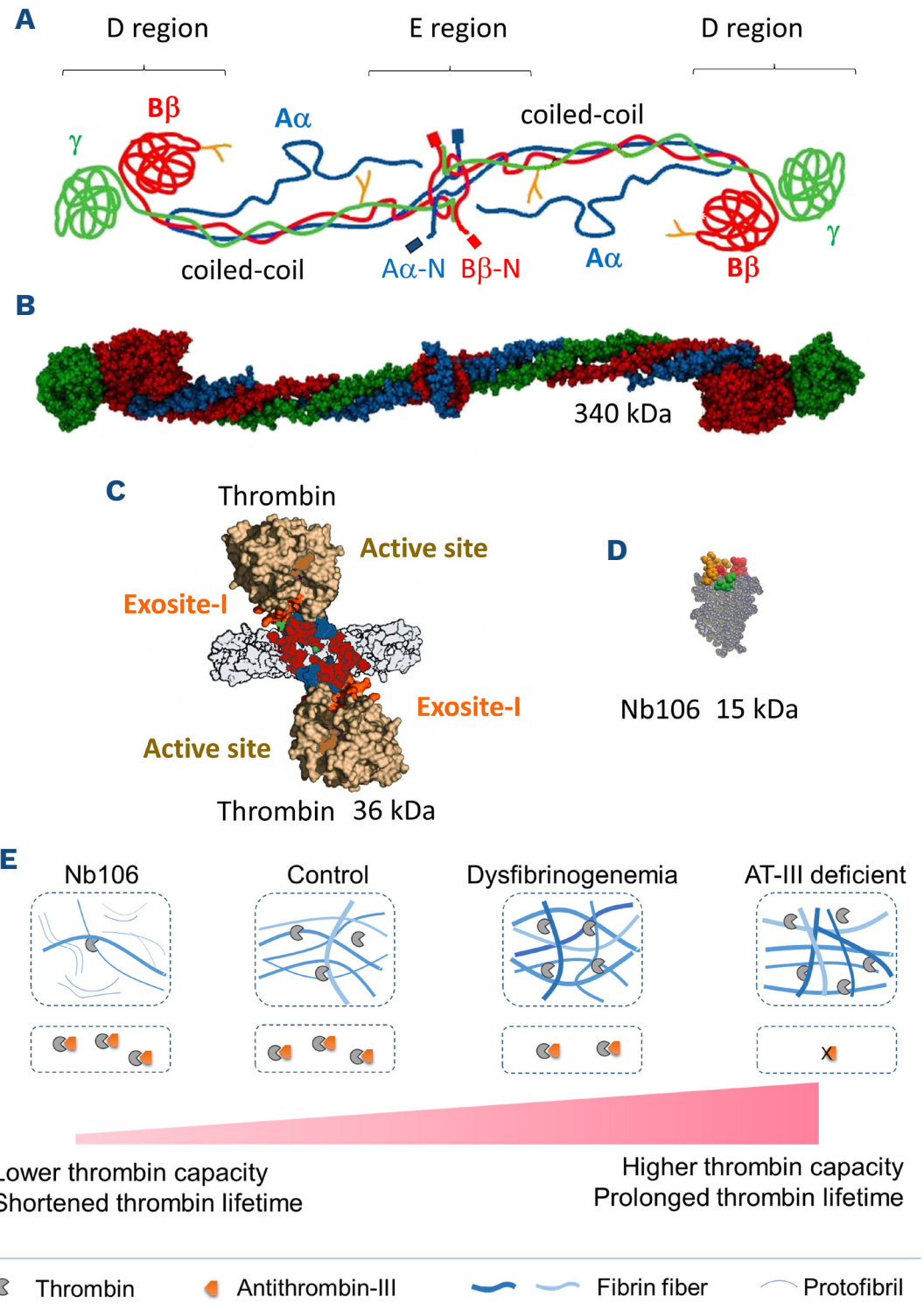

Figure 7. Schematized thrombin-fibrin interaction. (A, B) Cartoons of human fibrinogen, adapted from Köhler *et al*. 2015[44]. (A) Duplicate proteins chains Aα, Bβ and γ in 1 fibrinogen molecule are represented in blue, red and green colors, respectively. Indicated are the D-E-D regions connected by coiled-coil regions. Represented is a molecule with single N-terminally thrombin-cleaved Aα and Bβ chains producing an FpA and FpB peptide. (B) Corresponding space-filled model based on the crystal structure of fibrinogen, also lacking FpA and FpB (PDB: 3GHG). (C) Drawing modified from the crystal structure of a fibrin central E region in complex with 2 thrombin molecules (PDB: 2A45). Central parts of the Aα, Bβ and γ chains are represented in blue, red and green color, respectively. Gray area represent coiled-coil region. Attached thrombin molecules are shown in beige, with the active site in mustard, and exosite-I in orange. Adapted from Pechik *et al*.[13] (D) Global structure of a single chain antibody as model for Nb106. In colors, the 3 complementarity determining regions (CDR1-3) determining selective target (modified after Jacksonimmuno.com/camelid). (E) Proposed model of thrombin-fibrin interactions in the presence of Nb106, in normo- and dysfibrinogenemia or antithrombin-III deficiency, globally linked to thrombin activity.

and a risk of thrombophilia, considering that the overall low fibrinogen antigen levels can also result in bleeding phenotype. Our hypothesis with respect to severe dysfibrinogenemia is that an imperfect alignment of the fibrin Aα and Bβ chains keeps thrombin connected to the growing fibrin fibers, temporarily preventing its inactivation by antithrombin-III (Figure 7E). This idea was further supported by the increased thrombin activity observed by Pep1 corresponding to the N-terminal Aα chain. In this respect, fibrin as a previously assigned antithrombin-I, differs from antithrombin-III in that it keeps thrombin active in the proteolytic cleavage of substrates like fibrinogen molecules.

In conclusion, thrombin binding to fibrin, displaced by Nb106 and altered in cases of dysfibrinogenemia, regulates not only lateral fibrillar extension, but also provides protection against antithrombin-III inactivation. Constructs of Nb106 and fibrin Aα/Bβ-derived peptides may provide novel anti- and procoagulant treatment options for thrombosis and hemostasis, respectively.

Disclosures

BdL, JK, DH, SS, HM and MR are employees of the Synapse Research Institute Maastricht (member of the Stago Diagnostic group). PGdG and JWMH are advisors of the same institute. All other authors have no conflicts of interest to disclose.

Contributions

SS, MR, PGdG, EC, SB, PO and JWMH contributed to study design, data interpretation and manuscript writing. SS, RTU, CB, SDC, TF, DH, JK, RM, HM and PO contributed to data generation and analysis. EC, RM, AC and PS contributed to patient inclusion and clinical data evaluation. RM, BN, RASA, AC, PS, PGdG, JWMH and BdL contributed to material generation, supervision, and manuscript editing.

Acknowledgments

The authors are grateful to Dr. Jun Wan for his technical assistance with thrombin generation assessments and to Dr. Cuicui Bai for her help with the preparation and purification of PPACK-thrombin.

Funding

This work was supported in part by the China Scholarship Council (CSC, grant number 201906220218) (to SS).

Data-sharing statement

Correspondence for material requests should be addressed to the corresponding author. For Supplementary Material for this paper, see the Online Supplementary Appendix. All data supporting the present study are provided in the manuscript and the Online Supplementary Appendix.

References

1. Macfarlane RG. An enzyme cascade in the blood clotting mechanism, and its function as a biochemical amplifier. Nature. 1964;202:498-499.
2. Hoffman M, Monroe DM. A cell-based model of hemostasis. Thromb Haemost. 2001;85(6):958-965.
3. Furie B, Furie BC. Mechanisms of thrombus formation. N Engl J Med. 2008;359(9):938-949.
4. Mann KG, Brummel K, Butenas S. What is all that thrombin for? J Thromb Haemost. 2003;1(7):1504-1514.
5. Versteeg HH, Heemskerk JW, Levi M, Reitsma PH. New fundamentals in hemostasis. Physiol Rev. 2013;93(1):327-358.
6. Sang Y, Roest M, de Laat B, de Groot PG, Huskens D. Interplay between platelets and coagulation. Blood Rev. 2021;46(1):100733.
7. Hantgan RR, Simpson-Haidaris PJ, Francis CW, Marder VJ. Fibrinogen structure and physiology. In: Colman RW, Clowes AW, George JN, Goldhaber SZ, Marder VJ, editors. Hemostasis and thrombosis: basic principles and clinical practice. Philadelphia (PA): Lippincott Williams & Wilkins; 2001. p. 203-232.
8. Soya K, Terasawa F, Okumura N. Fibrinopeptide A release is necessary for effective B:b interactions in polymerisation of variant fibrinogens with impaired A:a interactions. Thromb Haemost. 2013;109(2):221-228.
9. McDonagh J. Dysfibrinogenemia and other disorders of fibrinogen structure and function. In: Colman RW, Clowes AW, George JN, Goldhaber SZ, Marder VJ, editors. Hemostasis and thrombosis: basic principles and clinical practice. Philadelphia (PA): Lippincott Williams & Wilkins; 2001. p. 855-892.
10. Mosesson MW. Fibrinogen and fibrin structure and functions. J Thromb Haemost. 2005;3(8):1894-1904.
11. Weisel JW, Litvinov RI. Mechanisms of fibrin polymerization and clinical implications. Blood. 2013;121(10):1712-1719.
12. Wolberg AS, Sang Y. Fibrinogen and factor XIII in venous thrombosis and thrombus stability. Arterioscler Thromb Vasc Biol. 2022;42(8):931-941.
13. Pechik I, Madrazo J, Mosesson MW, Hernandez I, Gilliland GL, Medved L. Crystal structure of the complex between thrombin and the central E region of fibrin. Proc Natl Acad Sci U S A. 2004;101(9):2718-2723.
14. Macrae FL, Swieringa F, Heemskerk JW, Ariëns RA. High fibrinogen g' levels in patient plasma increase clot formation at arterial and venous shear rate. Blood Adv. 2021;5(17):3468-3477.
15. Smith GF. Fibrinogen-fibrin conversion. The mechanism of fibrin-polymer formation in solution. Biochem J. 1980;185(1):1-11.
16. Marchi R, Neerman-Arbez M, Gay V, et al. Comparison of different activators of coagulation by turbidity analysis of hereditary dysfibrinogenemia and controls. Blood Coagul Fibrinolysis. 2021;32(2):108-114.
17. Vanschoonbeek K, Feijge MA, van Kampen RJ, et al. Initiating and potentiating role of platelets in tissue factor-induced thrombin generation in the presence of plasma: subject-dependent variation in thrombogram characteristics. J Thromb Haemost. 2004;2(3):476-484.
18. Sun S, Campello E, Zou J, et al. Crucial roles of red blood cells and platelets in whole blood thrombin generation. Blood Adv. 2023;7(21):6717-6731.
19. Allan P, Uitte de Willige S, Abou-Saleh RH, Connell SD, Ariëns RA. Evidence that fibrinogen γ' directly interferes with protofibril growth: implications for fibrin structure and clot stiffness. J Thromb Haemost. 2012;10(6):1072-1080.

20. Beck S, Öftering P, Li R, et al. Platelet glycoprotein V spatio-temporally controls fibrin formation. Nat Cardiovasc Res. 2023;2(4):368-382.
21. Brouns S, van Geffen JP, Campello E, et al. Platelet-primed interactions of coagulation and anticoagulation pathways in flow-dependent thrombus formation. Sci Rep. 2020;10(1):11910.
22. Rühl H, Müller J, Harbrecht U, et al. Thrombin inhibition profiles in healthy individuals and thrombophilic patients. Thromb Haemost. 2012;107(5):848-853.
23. Pandya BV, Gabriel JL, O'Brien J, Budzynski AZ. Polymerization site in the beta chain of fibrin: mapping of the B beta 1-55 sequence. Biochemistry. 1991;30(1):162-168.
24. Moskowitz KA, Budzynski AZ. The (DD)E complex is maintained by a composite fibrin polymerization site. Biochemistry. 1994;33(42):12937-12944.
25. McDonagh RP, Carrell NA, Roberts HR, Blatt PM, McDonagh J. Fibrinogen Chapel Hill: hypodysfibrinogenemia with a tertiary polymerization defect. Am J Hematol. 1980;9(1):23-38.
26. Crossen J, Diamond SL. Thermal shift assay to probe melting of thrombin, fibrinogen, fibrin monomer, and fibrin: Gly-Pro-Arg-Pro induces a fibrin monomer-like state in fibrinogen. Biochim Biophys Acta Gen Subj. 2021;1865(2):129805.
27. Bai C, Konings J, Ninivaggi M, Lancé M, de Laat B, de Laat-Kremers R. Assessing the individual roles of FII, FV, and FX activity in the thrombin generation process. Front Cardiovasc Med. 2022;9:1000812.
28. Stobb MT, Neeves KB, Monroe DM, Sindi SS, Leiderman K, Fogelson AL. Mathematical modeling identifies clotting factor combinations that modify thrombin generation in normal and factor VIII-, IX-, or XI-deficient blood. Res Pract Thromb Haemost. 2024;8(7):102570.
29. Casini A, Moerloose P, Neerman-Arbez M. Clinical, laboratory, and molecular aspects of congenital fibrinogen disorders. Semin Thromb Hemost. 2025;51(2):103-110.
30. De Moerloose P, Casini A, Neerman-Arbez M. Congenital fibrinogen disorders: an update. Semin Thromb Hemost. 2013;39(6):585-595.
31. Zanetto A, Campello E, Bulato C, et al. Impaired whole blood thrombin generation is associated with procedure-related bleeding in acutely decompensated cirrhosis. J Hepatol. 2025;82(6):1023-1035.
32. Spiegelenberg JP, de Laat-Kremers R, Roest M, et al. Low thrombin inactivation capacity is associated with an increased risk of recurrent ischemic events after ischemic stroke at a young age. J Thromb Haemost. 2025;23(3):978-988.
33. Hsieh KH. Localization of an effective fibrin beta-chain polymerization site: implications for the polymerization mechanism. Biochemistry. 1997;36(31):9381-9387.
34. Hsieh K. Thrombin interaction with fibrin polymerization sites. Thromb Res. 1997;86(4):301-316.
35. Becker DL, Fredenburgh JC, Stafford AR, Weitz JI. Exosites 1 and 2 are essential for protection of fibrin-bound thrombin from heparin-catalyzed inhibition by antithrombin and heparin cofactor II. J Biol Chem. 1999;274(10):6226-6233.
36. Siebenlist KR, DiOrio JP, Budzynski AZ, Mosesson MW. The polymerization and thrombin-binding properties of des-(B beta 1-42)-fibrin. J Biol Chem. 1990;265(30):18650-18655.
37. Wolberg AS, Campbell RA. Thrombin generation, fibrin clot formation and hemostasis. Transfus Apher Sci. 2008;38(1):15-23.
38. Huntington JA. Natural inhibitors of thrombin. Thromb Haemost. 2014;111(4):583-589.
39. Marar TT, Matzko CN, Wu J, et al. Thrombin spatial distribution determines protein C activation during hemostasis and thrombosis. Blood. 2022;139(12):1892-1902.
40. Berny MA, Munnix IC, Auger JM, et al. Spatial distribution of factor Xa, thrombin, and fibrin(ogen) on thrombi at venous shear. PLoS One. 2010;5(3):e10415.
41. Casini A, de Moerloose P. How I treat dysfibrinogenemia. Blood. 2021;138(21):2021-2030.
42. Sugo T, Endo H, Matsuda M, et al. A classification of the fibrin network structures formed from the hereditary dysfibrinogens. J Thromb Haemost. 2006;4(8):1738-1746.
43. Marchi R, Vilar R, Durual S, et al. Fibrin clot properties to assess the bleeding phenotype in unrelated patients with hypodysfibrinogenemia due to novel fibrinogen mutations. Thromb Res. 2021;197(1):56-64.
44. Köhler S, Schmid F, Settanni G. The internal dynamics of fibrinogen and its implications for coagulation and adsorption. PLoS Comp Biol. 2015;11(7):e1004346.